# Multi-scale investigation of dislocation mediated carbon migration in iron

Tigany Zarrouk

July 12, 2020

## Contents

### Abstract

We investigate the validity of a dislocation-assisted carbon migration mechanism underpinning the formation of dark etching regions in bearing steels undergoing high-cycle fatigue through use of a multi-scale approach: from quantum mechanics, to stochastic simulations. We start from tight binding simulations of $1/3\langle 111\rangle$ screw dislocations to obtain the 2-d Peierls potential and Fe-C binding energies. These become ingredients for a line-tension model of the $1/3\langle 111\rangle$ screw dislocation to obtain the kink-pair formation energy as a function of stress and carbon concentration. Finally, 3-d kinetic Monte-Carlo simulations of dislocations in an environment of carbon are used to ascertain which temperature and stress regimes dislocation-assisted carbon migration is a valid mechanism.

## 1   Introduction

## 2   Computational Method

- Use tight-binding model of Paxton and Elsaetter [1].

- Generate dislocations using anisotropic elasticity theory.

- Create clusters of dislocations in both easy and hard core configurations.

- Place carbon in octahedral sites around the core

- Calculate corrections (ZPE etc)

# 3  Results

## 3.1  Peierls Potential

To determine the Peierls potential, we followed the procedure detailed in Itakura [2]. Quadrupolar arrays of dislocations were constructed by placing dislocations of antiparallel $1/2\langle 111\rangle$ Burgers vectors in an "S" arrangement [3], with initial displacements determined by the anisotropic elasticity solutions. These displacements were modified to be periodic, thereby removing artificial stacking faults which would appear between periodic images after the introduction of the dipole. This was achieved by the subraction of a linear error term from the superposition of displacement fields arising from the dislocations in the simulation cell and its periodic images [4]. To accomodate for the internal stress upon introduction of the dislocation dipole into a simulation cell, an elastic strain was imposed on the cell, resulting in an extra tilt component being added to the cell vectors [3, 4]. Simulation cells were constructed with different initial core positions, which were sampled from the triangular region "EHS" (easy, hard and split) core positions, as detailed in 1. To fix the dislocation positions during relaxation, the three atoms surrounding the easy core, for each dislocation, were fixed during relaxation.

The interaction energy between the dislocation dipole and periodic images followed the prescription of Bulatov and Cai [4]. In isotropic elasticity, the elastic energy of a single dislocation dipole in an infinite lattice is given by

$$E_{\mathrm{el}}^{\mathrm{inf}} = \frac{\mu b^2}{4\pi} ln(\frac{r}{r_c})$$

The contribution from periodic images to the correction is

$$E_{\mathrm{img}} = E_{\mathrm{el}}(\mathbf{a}, \mathbf{c}_i, r_c) - E_{\mathrm{el}}^{\mathrm{inf}}(\mathbf{a}, r_c)$$

,

where

$$E_{\mathrm{img}} = \sum_{\mathbf{R}}' E_{\mathrm{dd}}(\mathbf{R}),$$

where $\mathbf{R}$ is a sum over dislocation dipoles in the periodic images exclusively.

$$E_{\mathrm{dd}}(\mathbf{R}) = \frac{\mu b^2}{2\pi} \ln \frac{|\mathbf{R}|^2}{|\mathbf{R} + \mathbf{a}| \cdot |\mathbf{R} - mathbf a|}$$

"Ghost" dipoles are introduced to account for the conditional convergence of the sum at $\pm\alpha\mathbf{b}$ and $\pm\beta\mathbf{b}$, where $\alpha = \beta = 0.5$.

As dislocations were kept at the same distance for each calculation, the difference in interaction energies, with dipole correction, was negligible.

Comparison of 2d Peierls potentials of the $1/2\langle 111\rangle$ screw dislocation between DFT can by found in [2]. Data was interpolated using 2d cubic splines. "E", "H" and "S" correspond to easy, hard and split core positions respectively, with the latter also corresponding to atomic positions. The relative energies between the different core positions is smaller in tight-binding compared to DFT; most notably, the energies. This is an artifact in the model, which has been validated in NEB calculations of the $1/2\langle 111\rangle$ screw dislocation Peierls barrier, as calculated with NEB, is roughly half that when compared to DFT **INSERT**
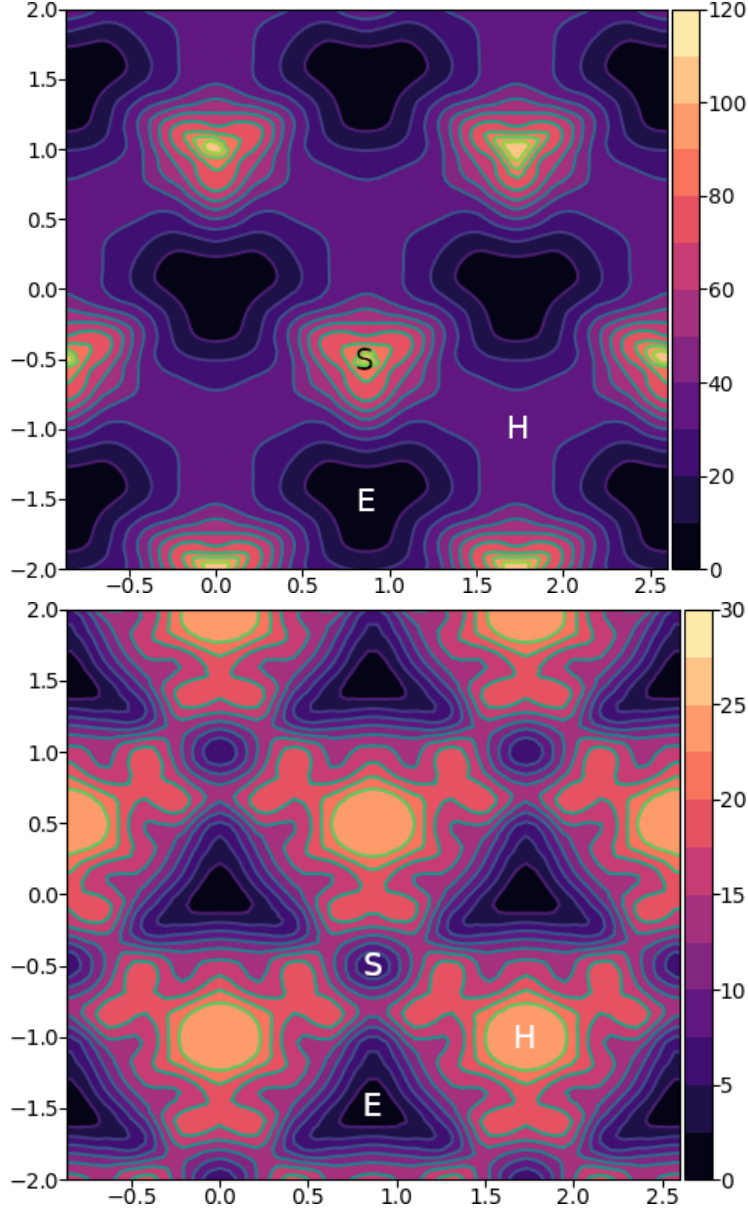
Table 1: Comparison of 2d Peierls potentials of the $1/2\langle111\rangle$ screw dislocation between DFT cite:Itakura2012 (top) and tight-binding (bottom). Data was interpolated using cubic splines. Energies are in $meV$, with x and y scales in units of $\sqrt{2}a_{\mathrm{bcc}} = 2\sqrt{2/3}b$. "E", "H" and "S" correspond to easy, hard and split core positions respectively, with the latter also corresponting to atomic positions. The relative energies between the different core positions is smaller in tight-binding compared to DFT. The split core as seen in tight-binding is reminiscent of EAM potentials, where the split core energy is lower than that of the hard core. Some of this discrepancy can be attributed to the difference in simulation method: the cluster method may inhibit the relaxation of the core more than quadrupolar cells, due to finite size effects.

3

**LUKES THESIS REFERENCE**. The split core as seen in tight-binding is reminiscent of EAM potentials, where the split core energy is lower than that of the hard core.

This may be attributed to lack of core electron repulsion, resulting from the sd-iron tight-binding model.

| Pos | $\Delta E_{\mathrm{INT}}$ | $\Delta E_{\mathrm{tbe}}$ | $\Delta E_{\mathrm{P}}$ | $\Delta E_{\mathrm{P}}^{\mathrm{DFT}}$ |
|---|---|---|---|---|
| 1 | 0 | 0 | 0 | 0 |
| 2 | -0.7 | 7.3 | 7.9 | 3.2 |
| 3 | -1.4 | 16.0 | 17.4 | 19.2 |
| 4 | -2.0 | 22.2 | 24.2 | 31.1 |
| 5 | -2.5 | 24.8 | 27.4 | 39.3 |
| 6 | -3.3 | 3.0 | 6.3 | 11.5 |
| 7 | -6.5 | 7.1 | 13.6 | 39.9 |
| 8 | -9.6 | 13.0 | 22.6 | 75.2 |
| 9 | -12.5 | 5.4 | 17.9 | 108.9 |
| 10 | -4.8 | 22.1 | 26.9 | 34.8 |
| 11 | -7.2 | 18.2 | 25.4 | 37.9 |
| 12 | -9.8 | 14.0 | 23.8 | 60.7 |
| 13 | -3.8 | 11.5 | 15.3 | 17.6 |
| 14 | -6.9 | 15.1 | 22.0 | 29.9 |
| 15 | -4.3 | 18.6 | 22.9 | 39.7 |

## 3.2   Hard and easy core relaxations

To determine the binding energy of carbon to dislocations, we used the cluster method; where the simulation cells consist of a circular cluster of atoms, split into two regions, with a single dislocation introduced into the centre by using the anisotropic elasticity solutions. Each of the clusters were centred on the easy or hard core positions. The cluster of atoms was split into two regions: a central region of dynamic atoms with radius $R_1$, and an annulus of atoms, between $R_1$ and $R_2$, which were fixed to the anisotropic elasticity solutions.

Initially, large cells of with $R_1 = 6\sqrt{2}a_{\mathrm{bcc}}$, and $R_2 = 7\sqrt{2}a_{\mathrm{bcc}}$ and depth of single burger's vector, were relaxed for both the easy and hard cores, which consisted of 522 and 540 atoms respectively. The three atoms surrounding the core were constrained, to only relax in $X-Y$ plane, to stop the core from moving upon relaxation. The k-point sampling mesh for each of these cells was 1x1x24, with a charge tolerance for self-consistency of $1e-6$. Atoms were relaxed until the force on each atom was less than $1e-3$ eV/Å.

From the relaxed cells, a smaller region of 174 atoms, with $R_1 = 3\sqrt{2}a_{\mathrm{bcc}}$, and $R_2 = 4\sqrt{2}a_{\mathrm{bcc}}$, was cut from the dynamic regions. This smaller cell was extended to a thickness of 3b in the Z direction. Carbon interstitials were inserted into octahedral sites near the dislocation core, in the middle layer. Exploiting reflection and rotational symmetry, allows us to use only 10 interstitial sites to obtain the binding energies of carbon $\sim 1.8$ b from the core.

The three atoms surrounding the core on the first and third layers were again constrained to relax only in the $X$ and $Y$ directions. No such constraints were imposed on the middle layer.

As found in DFT simulations by Ventelon [5], when a carbon was placed in the vicinity of a relaxed easy dislocation core—in either of the two nearest,

distinguishable, octahedral sites—a spontaneous reconstruction of the dislocation core occurred: from easy to hard. Upon reconstruction, the dislocation core moved to a neighbouring triangle, when looking along the $\langle 111 \rangle$ direction, where the carbon found itself situated in the centre.

Plot of dislocation energy as function of cluster size.
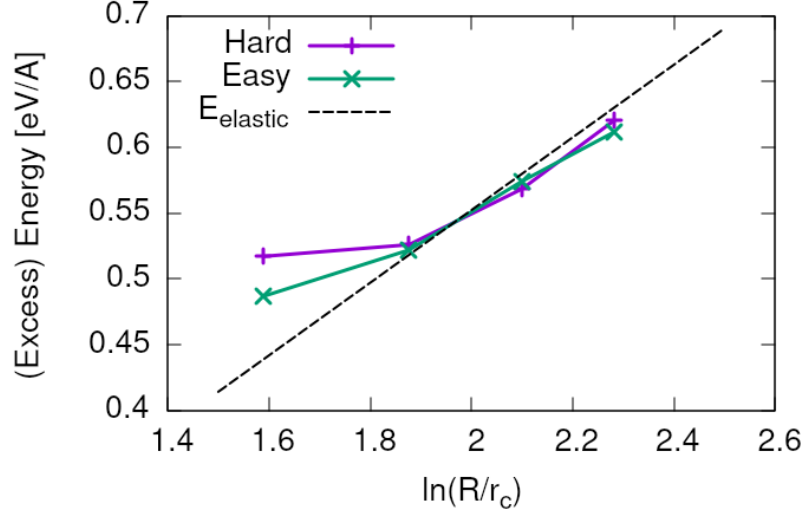


Following the paper by Itakura [6] we calculated the binding energy of carbon each of the screw dislocation cores.

The solution energy is given by

$$E_s = E_{d + C} - E_d - E_{C \ ref.},$$

where $E_{d + C}$ is the total energy of a relaxed cluster with a carbon interstitial and a dislocation, $E_d$ is the total energy of a relaxed cluster with a dislocation and $E_{C \ oct.}$ is the total energy of relaxed a cluster with a single carbon in an octahedral site.

The zero-point energy is calculated as in Itakura. After relaxation of the C-dislocation system, a 3x3 Hessian matrix is constructed by taking the numerical derivative of forces observed on the carbon atom after displacement by $\pm 0.015$ in each of the $X$, $Y$ and $Z$ directions. The three atoms surrounding the core on the first and third layers were again fixed in $Z$ coordinate. The zero-point energy is given by

$$E_z = \frac{1}{2} \sum_{i=1}^{3} \frac{h}{2\pi} \sqrt{k_i/m_C},$$

where $k_i$ are the eigenvalues of the Hessian and $m_C$ is the mass of carbon.

The ZPE corrected solution energy is given by

$$E_s^Z = E_s + \Delta E_z,$$

where $\Delta E_z = E_z - E_{zC \ ref.}$ and $E_{zC \ ref.} = 202.5 meV$ is the zero-point energy of carbon situated in an octahedral site in a perfect cluster of the same size.
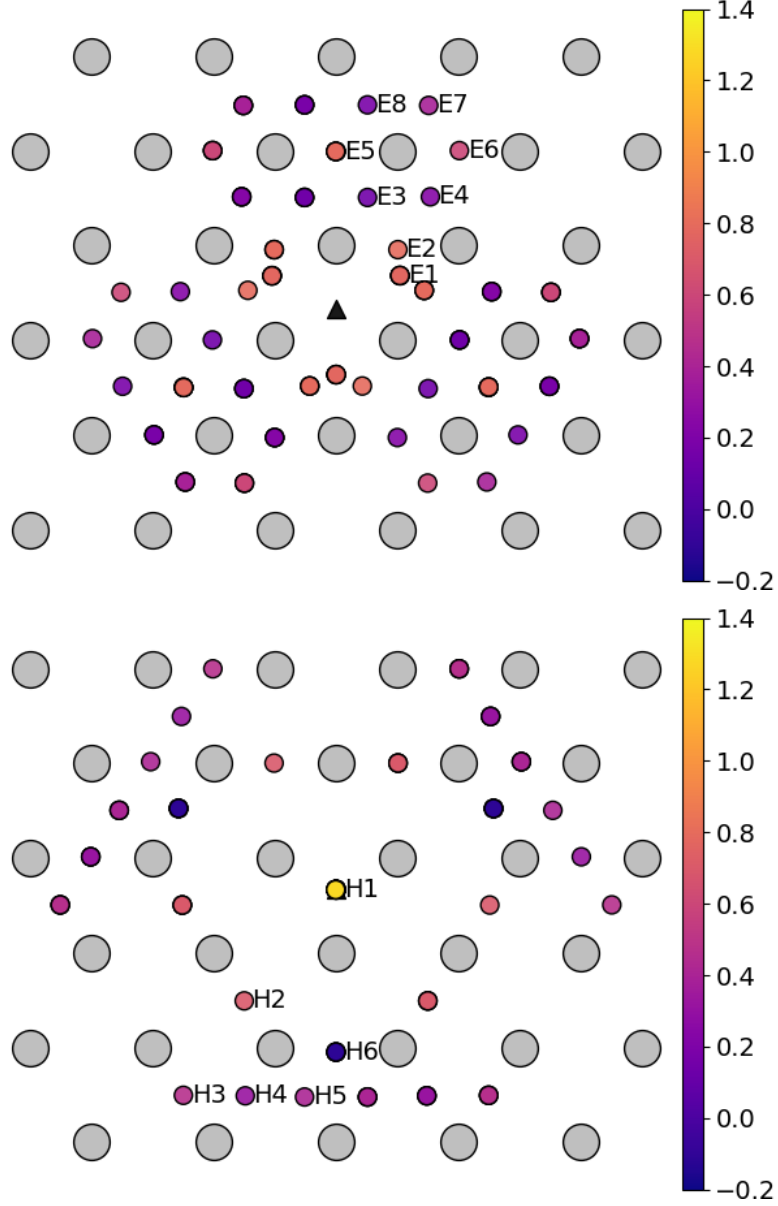
Table 2: Final positions and binding energies (eV) of carbon around the easy core (top) and hard core (bottom). The core was constrained by fixing the top and bottom three atoms surrounding each of the cores. As shown by Ventelon cite:Ventelon2015, the first and second closest octahedral sites to the hard core have their minimum energy inside the hard core.

| Site Type | distance from core [b] | $E^z$ [eV] | $\Delta E^z$ [eV] | $E_b$ [eV] | $E_b^z$ [eV] |
|-----------|------------------------|------------|-------------------|------------|--------------|
| E1 | 0.57 | 0.185 | -0.018 | 0.793 | 0.775 |
| E2 | 0.70 | 0.202 | -0.001 | 0.793 | 0.793 |
| E3 | 0.99 | 0.205 | 0.002 | 0.137 | 0.139 |
| E4 | 1.21 | 0.208 | 0.005 | 0.229 | 0.234 |
| E5 | 1.36 | 0.210 | 0.008 | 0.784 | 0.791 |
| E6 | 1.66 | 0.209 | 0.007 | 0.597 | 0.603 |
| E7 | 1.89 | 0.206 | 0.003 | 0.385 | 0.388 |
| E8 | 1.77 | 0.203 | 0.000 | 0.177 | 0.178 |
| H1 | 0.00 | 0.196 | -0.006 | 1.298 | 1.291 |
| H2 | 1.19 | 0.210 | 0.007 | 0.691 | 0.698 |
| H3 | 2.12 | 0.209 | 0.007 | 0.461 | 0.467 |
| H4 | 1.91 | 0.207 | 0.005 | 0.311 | 0.316 |
| H5 | 1.80 | 0.208 | 0.006 | 0.403 | 0.409 |
| H6 | 1.40 | 0.207 | 0.005 | -0.119 | -0.114 |

Table 3: Table of energies leading to the zero-point energy corrected binding energy.


These binding energies agree well with experiment and previous calculations. The maximum binding energy found by the Fe-C EAM potential by Becquart [7], was 0.41eV. Kamber *et al.* found a maximum binding energy of 0.5 eV. Cochardt found a value of 0.71 eV, which is within 0.1eV of the largest binding energy for the easy core.

Distance dependence of binding energies.
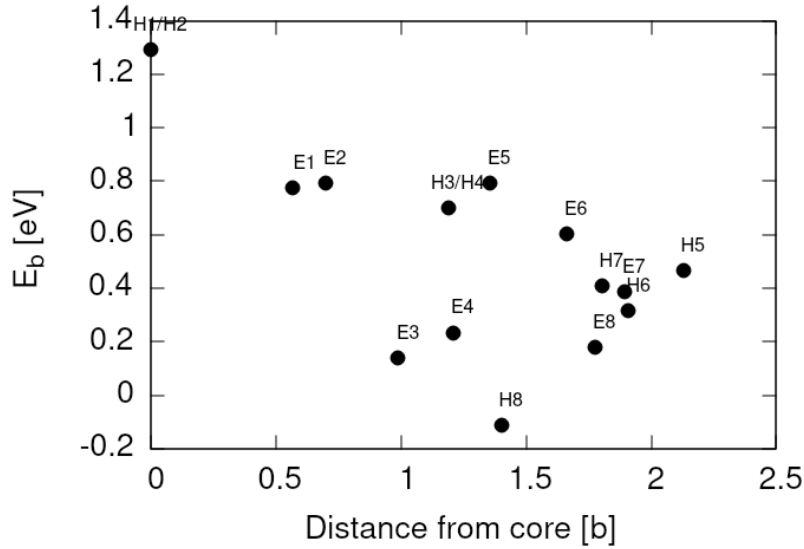
# 4 Bibliography

## References

[1] A. T. Paxton and C. Elsässer. Analysis of a carbon dimer bound to a vacancy in iron using density functional theory and a tight binding model. *Physical Review B*, 87(22), June 2013.

[2] M. Itakura, H. Kaburaki, and M. Yamaguchi. First-principles study on the mobility of screw dislocations in bcc iron. *Acta Materialia*, 60(9):3698–3710, May 2012.

[3] Emmanuel Clouet. Screw dislocation in zirconium: An ab initio study. *Physical Review B - Condensed Matter and Materials Physics*, 86(14):1–11, 2012.

[4] Vasily Bulatov. *Computer Simulations of Dislocations (Oxford Series on Materials Modelling)*. Oxford University Press, dec 2006.

[5] Lisa Ventelon, B. Lüthi, E. Clouet, L. Proville, B. Legrand, D. Rodney, and F. Willaime. Dislocation core reconstruction induced by carbon segregation in bcc iron. *Physical Review B*, 91(22), June 2015.

[6] M. Itakura, H. Kaburaki, M. Yamaguchi, and T. Okita. The effect of hydrogen atoms on the screw dislocation mobility in bcc iron: a first-principles study. *Acta Materialia*, 61(18):6857–6867, 2013.

[7] C.S. Becquart, J.M. Raulot, G. Bencteux, C. Domain, M. Perez, S. Garruchet, and H. Nguyen. Atomistic modeling of an fe system with a small concentration of c. *Computational Materials Science*, 40(1):119–129, July 2007.